

Higgs boson phenomenology in a simple model with vector resonances

Oscar Castillo-Felisola^{1,2}, Cristóbal Corral^{1,2}, Marcela González^{1,2}, Gastón Moreno^{1,2}, Nicolás A. Neill^{1,2}, Felipe Rojas^{1,2}, Jilberto Zamora^{1,2}, Alfonso R. Zerwekh^{1,2,a}

¹Departamento de Física, Universidad Técnica Federico Santa María, Casilla 110-V, Valparaíso, Chile

²Centro Científico-Tecnológico de Valparaíso, Universidad Técnica Federico Santa María, Casilla 110-V, Valparaíso, Chile

Received: 8 August 2013 / Revised: 30 October 2013 / Published online: 6 December 2013
© Springer-Verlag Berlin Heidelberg and Società Italiana di Fisica 2013

Abstract In this paper we consider a simple scenario where the Higgs boson and two vector resonances are supposed to arise from a new strong interacting sector. We use the ATLAS measurements of the dijet spectrum to set limits on the masses of the resonances. Additionally we compute the Higgs boson decay to two photons and found, when compare to the Standard Model prediction, a small excess which is compatible with ATLAS measurements. Finally we make prediction for Higgs-strahlung processes for the LHC running at 14 TeV.

1 Introduction

The 125 GeV Higgs boson recently discovered at the LHC [1, 2] seems to behave in a very standard way. No important deviation from the Standard Model (SM) predictions has been found except for a small discrepancy in its decay to two photons which still survives in ATLAS measurements. As a result, stringent constraints have been put on an eventual New Physics at the TeV scale. The Minimal Supersymmetric Standard Model (MSSM), for instance, seems to suffer from serious tensions trying to accommodate simultaneously such a large mass for the lighter Higgs boson and the current non-observability of any “super-partner” at the TeV scale. Indeed, the current exploration of supersymmetric alternatives to the Standard Model, in general, seems to need a structure that goes beyond the minimal possibility [3]. On the other hand, the LHC has evidently ruled out a complete family of Dynamical Electroweak Symmetry Breaking (DEWSB) models which predicted a Higgsless low energy spectrum. Nevertheless, there are some classes of DEWSB models which predict a light composite Higgs boson and

still offer a viable explanation for the stability of the Electroweak scale. For instance, Walking Technicolor (WTC) [4, 5]¹ (although it is still not clear whether a composite scalar as light as 125 GeV is possible, see for example, Ref. [7]) and models where the Higgs is a pseudo-Goldstone boson are notable examples of such kind of models with a light scalar in the spectrum [8–24].

In this paper, we consider a hypothetical scenario where it is assumed that a new strong interacting sector originates the Fermi scale and manifests itself by means of a composite scalar boson (which we identify with the 125 GeV Higgs boson) and vector resonances. In order to make this scenario concrete, we use a simple phenomenological model proposed by one of us some years ago [25]. In this model, two kind of vector resonances are included: a triplet of $SU(2)_L$ (which can be thought of as a “techni-rho” and then we denote it by ρ_μ) and a singlet of $SU(2)_L$ (which can be thought of as a “techni-omega” and then we denote it by ω_μ). It is assumed that these new states interact with the particles of the SM by their mixing with the standard gauge bosons W_μ^a and B_μ in analogy to the well known Vector Meson Dominance (VMD) mechanism in Hadron Physics. Originally, this setup was used to point out that in a Composite Higgs framework an enhancement of the associate production of a Higgs and a gauge boson could be expected. This result, was later confirmed by other authors in the context of Minimal Walking Technicolor (MWTC) [26]. It has also been shown that MWTC also predicts a deviation of the Higgs to two photons decay ratio, compared with the SM. One of the main objectives of this work is to update the predictions presented in [25] which, as it was explained above, was one of the first phenomenological studies of a light composite Higgs eventually generated by an underlying technicolor sector. It must also be emphasized that, although the influence of

^a e-mail: alfonso.zerwekh@usm.cl

¹For a recent review of modern DEWSB models see [6].

new spin-1 fields on the Higgs sector has been studied by many authors (for recent examples see Refs. [27–33]), here we try to present a simple scenario where the scalar sector is kept minimal while we propose a “traditional” technicolor spectrum of composite spin-1 resonance. The inclusion of a techni-omega, for instance, is important for the prediction of the $pp \rightarrow Zh$ channel.

In this work, we use the simple framework described above and data from the ATLAS Collaboration to set limits on the masses of the vector resonances. Additionally, we make some predictions for the next run of the LHC. Finally, based on our results, we comment on some characteristics we think must be respected by DEWSB scenarios.

The paper is organized in the following way. In Sect. 2 we describe the theoretical construction. Section 3 is devoted to set limits on the mass of the resonances based on dijet measurements. In Sect. 4 we evaluate the consistency of the model with the current measurement of $\Gamma(h \rightarrow \gamma\gamma)$. In Sect. 5 we compute Higgs-strahlung processes for the LHC at $\sqrt{s} = 14$ TeV. Finally, in Sect. 6 we comment our results and state our conclusions.

2 The model

The model studied in this work was already proposed elsewhere by one of us [25]. Nevertheless, in regard of the completeness, we dedicate this section to a presentation of the main characteristics of our theoretical construction.

2.1 Gauge sector

As explained above, our model contains two new vector fields which are supposed to be the manifestation of an underlying strong sector. We assume that these resonances interact with the standard sector through their mixing with the electroweak gauge bosons, following the VMD idea. In a more modern but equivalent language, the model can be formulated based on the “moose” diagram shown in Fig. 1.

The resulting low energy Lagrangian (assuming that the Abelian and non-Abelian parts break at the same scale) can

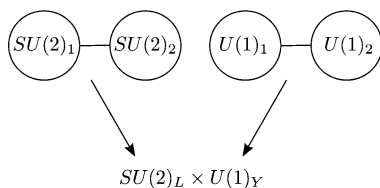


Fig. 1 Gauge structure of the model. Our construction may be thought of as coming from a moose diagram like the one shown here. The initial gauge symmetry $SU(2)_1 \times SU(2)_2 \times U(1)_1 \times U(1)_2$ is broken down (by a non-linear sigma sector, for example) to $SU(2)_L \times U(1)_Y$ and our effective Lagrangian (1) is obtained

be written as

$$\begin{aligned} \mathcal{L} = & -\frac{1}{2}\text{Tr}\{W_{\mu\nu}W^{\mu\nu}\} - \frac{1}{2}\text{Tr}\{\tilde{\rho}_{\mu\nu}\tilde{\rho}^{\mu\nu}\} \\ & - \frac{1}{4}B_{\mu\nu}B^{\mu\nu} - \frac{1}{4}\tilde{\omega}_{\mu\nu}\tilde{\omega}^{\mu\nu} \\ & + M^2\text{Tr}\left\{\left(\frac{g}{g_2}W_\mu - \tilde{\rho}_\mu\right)^2\right\} + \frac{M^2}{2}\left(\frac{g'}{g_2}B_\mu - \tilde{\omega}_\mu\right)^2, \end{aligned} \quad (1)$$

where W_μ and B_μ are the fields associated to the sites labeled by “1” while $\tilde{\rho}_\mu$ and $\tilde{\omega}_\mu$ are associated to the sites labeled by “2” and are assumed to be strongly coupled. As usual, $W_{\mu\nu}$, $\tilde{\rho}_{\mu\nu}$, $B_{\mu\nu}$ and $\tilde{\omega}_{\mu\nu}$ are (in terms of components)

$$W_{\mu\nu}^a = \partial_\mu W_\nu^a - \partial_\nu W_\mu^a + g\epsilon^{abc}W_\mu^bW_\nu^c, \quad (2)$$

$$\tilde{\rho}_{\mu\nu}^a = \partial_\mu \tilde{\rho}_\nu^a - \partial_\nu \tilde{\rho}_\mu^a + g_2\epsilon^{abc}\tilde{\rho}_\mu^b\tilde{\rho}_\nu^c, \quad (3)$$

$$B_{\mu\nu} = \partial_\mu B_\nu - \partial_\nu B_\mu, \quad (4)$$

$$\tilde{\omega}_{\mu\nu} = \partial_\mu \tilde{\omega}_\nu - \partial_\nu \tilde{\omega}_\mu. \quad (5)$$

By construction, Lagrangian (1) is invariant under $SU(2)_L \times U(1)_Y$. The symmetry breaking to $U(1)_{\text{em}}$ will be described by means of the vacuum expectation value of a scalar field, as in the Standard Model. In other words, we will use an effective gauged linear sigma model as a phenomenological description of the electroweak symmetry breaking.

2.2 Fermion sector

As usual, fermions are coupled to the gauge fields through covariant derivatives:

$$\mathcal{L} = \bar{\psi}_L i\gamma^\mu D_\mu \psi_L + \bar{\psi}_R i\gamma^\mu \tilde{D}_\mu \psi_R, \quad (6)$$

with

$$\begin{aligned} D_\mu = & \partial_\mu + i\tau^a g(1-x_1)W_\mu^a + i\tau^a g_2 x_1 \tilde{\rho}_\mu^a \\ & + i\frac{Y}{2}g'(1-x_2)B_\mu + i\frac{Y}{2}g'_2 x_2 \tilde{\omega}_\mu \end{aligned} \quad (7)$$

and

$$\tilde{D}_\mu = \partial_\mu + i\frac{Y}{2}g'(1-x_3)B_\mu + i\frac{Y}{2}g'_2 x_3 \tilde{\omega}_\mu. \quad (8)$$

The parameters x_i ($i = 1, 2, 3$) play the role of fermion delocalization [34] and in our case govern the direct coupling to the new vector bosons. In the context of the BESS model [35–40],² which shares with our model a similar

²For a review of effective models of a strong electroweak symmetry breaking sector with scalar and vector resonances, see [41].

structure in the spin-1 sector, it has been shown that a direct interaction of the order of $2(g/g_2)^2$ is necessary in order to reconcile the model with the precision electroweak parameters S , T and U . Hence, we adopt this result and impose $x_i = 2(g/g_2)^2$ for $i = 1, 2, 3$.

2.3 Higgs sector and EWSB

In our effective model, the Higgs sector is assumed to be the same as in the Standard Model except by the possibility of including a direct coupling, between the Higgs doublet and the vector resonances, depending on how the Higgs boson is localized. In this way, the Lagrangian for the Higgs sector can be written as

$$\mathcal{L} = (D^\mu \Phi)^\dagger (D_\mu \Phi) - V(\Phi), \quad (9)$$

where, as usual,

$$V(\Phi) = -\mu^2 \Phi^\dagger \Phi + \lambda (\Phi^\dagger \Phi)^2, \quad (10)$$

and

$$D_\mu = \partial_\mu + i\tau^a g(1 - f_1)W_\mu^a + i\tau^a g_2 f_1 \tilde{\rho}_\mu^a + i\frac{Y}{2}g'(1 - f_2)B_\mu + i\frac{Y}{2}g'_2 f_2 \tilde{\omega}_\mu. \quad (11)$$

For simplicity, we chose to completely localize the Higgs fields in the weakly coupled sites imposing $f_i = 0$ for $i = 1, 2$. The consequences of this choice will be discussed later.

Once the electroweak symmetry is broken, two non-diagonal mass matrices are generated: one for the neutral vector bosons and another for the charged one

$$\mathcal{M}_{\text{neutral}} = \frac{v^2}{4} \begin{bmatrix} (1 + \alpha^2)g^2 & -\alpha^2 g g_2 & -g g' & 0 \\ -\alpha^2 g g_2 & \alpha^2 g_2^2 & 0 & 0 \\ -g g' & 0 & (1 + \alpha^2)g'^2 & -\alpha^2 g' g_2 \\ 0 & 0 & -\alpha^2 g' g_2 & \alpha^2 g'^2 \end{bmatrix}, \quad (12)$$

$$\mathcal{M}_{\text{charged}} = \frac{v^2}{4} \begin{bmatrix} (1 + \alpha^2)g^2 & -\alpha^2 g g_2 \\ -\alpha^2 g g_2 & \alpha^2 g_2^2 \end{bmatrix}, \quad (13)$$

where

$$\alpha^2 = \frac{4M^2}{v^2 g_2^2}. \quad (14)$$

Notice that αv may be thought of as the scale where the mass of the rho and omega resonances is generated. It is natural to identify this scale with the natural scale of the strong sector which in our case is $\Lambda = 4\pi v$. Consequently,

we assume that the natural value of α is $\alpha = 4\pi$. Notice that Λ is also a natural upper limit for the value of the mass of the resonances. Additionally, we have assumed that the new vector resonances are degenerated in mass.

The mass matrices can be diagonalized and the eigenvectors, in the limit $g/g_2 \ll 1$ and keeping terms up to order g/g_2 , can be written as

$$\begin{aligned} A &= \frac{g'}{\sqrt{g^2 + g'^2}} W^3 + \frac{g}{\sqrt{g^2 + g'^2}} B \\ &\quad + \frac{g g'}{g_2 \sqrt{g^2 + g'^2}} \tilde{\rho}^3 + \frac{g g'}{g_2 \sqrt{g^2 + g'^2}} \tilde{\omega}, \\ Z &= \frac{g}{\sqrt{g^2 + g'^2}} W^3 - \frac{g'}{\sqrt{g^2 + g'^2}} B \\ &\quad + \frac{g^2}{g_2 \sqrt{g^2 + g'^2}} \tilde{\rho}^3 - \frac{g'^2}{g_2 \sqrt{g^2 + g'^2}} \tilde{\omega}, \end{aligned} \quad (15)$$

$$\rho^0 = -\frac{g}{g_2} W^3 + \tilde{\rho}^3,$$

$$\omega = -\frac{g'}{g_2} B + \tilde{\omega},$$

$$W^\pm = \tilde{W}^\pm + \frac{g}{g_2} \tilde{\rho}^\pm,$$

$$\rho^\pm = \tilde{\rho}^\pm - \frac{g}{g_2} \tilde{W}^\pm,$$

where

$$\tilde{W}^\pm = \frac{1}{\sqrt{2}} (W^1 \mp i W^2) \quad (16)$$

and

$$\tilde{\rho}^\pm = \frac{1}{\sqrt{2}} (\tilde{\rho}^1 \mp i \tilde{\rho}^2). \quad (17)$$

We used LanHEP [42] to implement this model into the CalcHEP package [43].

3 Limits from the dijet spectrum

As a first step, we proceed to obtain limits for the mass of the resonances using the dijet spectrum measured by ATLAS [44]. For this purpose, we generated events for the $pp \rightarrow jj$ process at $\sqrt{s} = 8$ TeV using CalcHEP, considering only the contribution of the new vector resonances. In order to compare with ATLAS data we imposed the following kinematic cuts:

$$\frac{1}{2} |y_1 - y_2| < 0.6, \quad (18)$$

$$|y_{1,2}| < 2.8, \quad (19)$$

$$M_{jj} > 1000 \text{ GeV}, \quad (20)$$

$$p_{T1,2} > 150 \text{ GeV}, \quad (21)$$

where y refers to the jet rapidity, p_T is the transverse momentum and M_{jj} is the invariant mass of the two jets. The main contribution to this process comes from the production of the ρ and ω in the s -channel through quark–anti-quark annihilation. Unfortunately, due to PDF effects, it is unlikely to produce anti-quarks with large momentum at the LHC and a considerable fraction of the events are produced in the low M_{jj} region. Of course, such events are hidden under the background. In consequence we select only the resonant part of our events in order to compare it with the experimental upper limits. For doing that, and after imposing the cuts, we fit the events around the resonant peak with a Breit–Wigner function and a second degree polynomial, describing the non-resonant “background”, and define our resonant events as the integral of the Breit–Wigner function. Now we are prepared to compare with experimental data. Our results are shown in Fig. 2. There, the ATLAS upper limits for invisible resonances are compared to our predicted cross section for dijet production considering only the contribution of the new vector fields and the appropriate kinematic cuts. Everything above the experimental curve is excluded. In our case, that means that our model is consistent with the ATLAS dijet measurements provided that the mass of the vector resonances satisfies the constrain $M \gtrsim 2200 \text{ GeV}$.

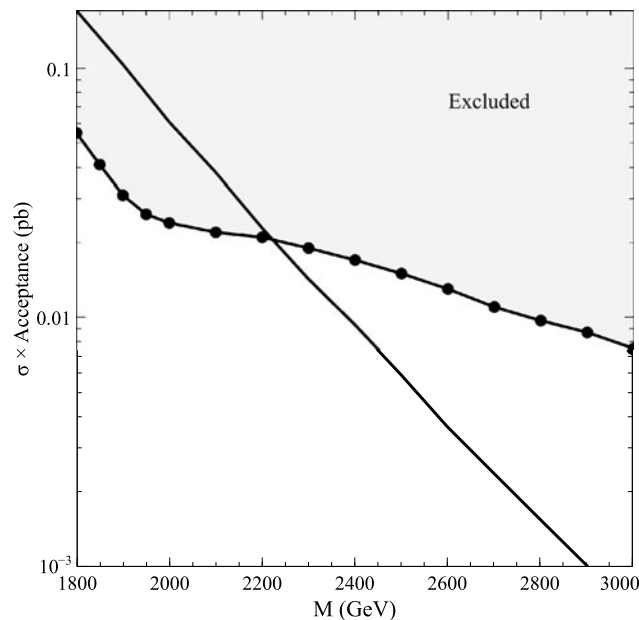


Fig. 2 Resonant cross sections (*continuous line*) compared to ATLAS upper limits to narrow resonances decaying into dijet (*dots with continuous line*), as a function of the resonance mass. The *colored region* is excluded

4 $h \rightarrow \gamma\gamma$

A relevant observable in Higgs phenomenology is its decay rate into two photons. This is the only measured quantity that presents a sensible deviation from the SM, at least in results reported by ATLAS. Since it is a loop effect, we expect that this observable is sensible to the existence of New Physics. With this motivation in mind, we computed the $\Gamma(h \rightarrow \gamma\gamma)$ in our model at one loop level. Non-standard contributions arise through the presence of the ρ_μ^\pm fields. The new diagrams are formally identical to those generated by the W_μ^\pm bosons except, obviously, by the different values of the coupling constants (which in case of the $h\rho^+\rho^-$ is suppressed by a factor $(g/g_2)^2$ with respect to hW^+W^-) and the vector boson masses. The result is shown in Fig. 3 where we have plotted the ratio

$$R_\gamma = \frac{\Gamma(h \rightarrow \gamma\gamma)_{\text{Model}}}{\Gamma(h \rightarrow \gamma\gamma)_{\text{SM}}} \quad (22)$$

as a function of the ρ mass. We see that in the allowed range of masses, R_γ varies from 1.25 to 1.50. This result has to be compared with the experimental values [45, 46]:

$$R_\gamma = \begin{cases} 1.6 \pm 0.3 & \text{ATLAS,} \\ 0.77 \pm 0.27 & \text{CMS.} \end{cases} \quad (23)$$

Notice that our results agree with the experimental values at 1σ level in the case of ATLAS and at 2.5σ level in the case of CMS.

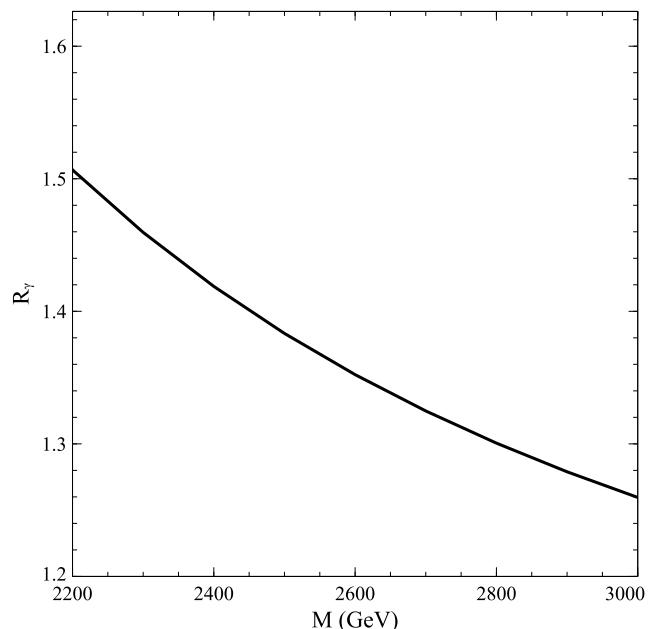


Fig. 3 Predicted values of $R_\gamma = \Gamma(h \rightarrow \gamma\gamma)_{\text{Model}} / \Gamma(h \rightarrow \gamma\gamma)_{\text{SM}}$

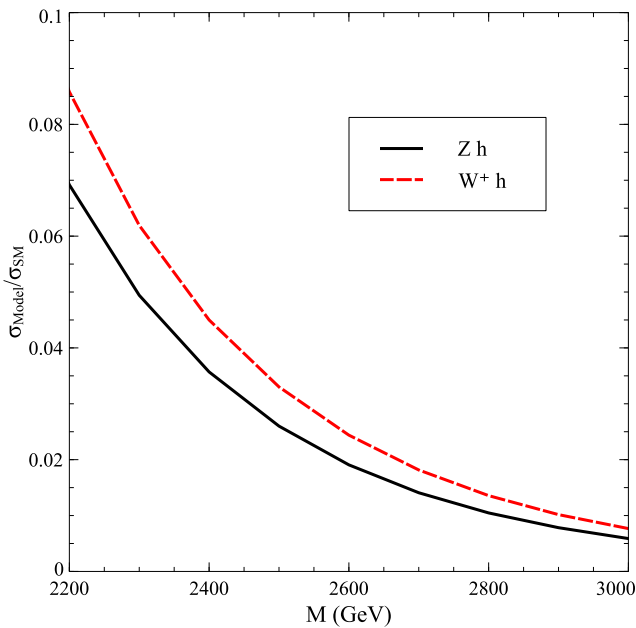


Fig. 4 Predicted cross sections for the processes $pp \rightarrow Zh$ (continuous line) and $pp \rightarrow W^+h$ (dashed line) at $\sqrt{s} = 14$ TeV due only to the contributions of the new spin-1 states compared to the SM prediction

5 Higgs strahlung

As explained above, the model studied in this paper was proposed by one of us some years ago. It was shown that for resonance masses that were reasonable at that time, the model presented a significant enhancement of associated production of a Higgs boson and a gauge boson. This result was confirmed later in the framework of the MWTC. Given this context, it is interesting to evaluate whether this channel remains a robust signal after considering the limits imposed by current experimental data. Consequently, we used CalcHEP to compute the cross sections for the processes $pp \rightarrow Zh$ and $pp \rightarrow W^+h$ at $\sqrt{s} = 14$ TeV due only to the contributions of the new spin-1 states and we compare it to the SM prediction. The result is shown in Fig. 4.

Unfortunately, our results show a very small enhancement in the cross section: less than 10 % in the available mass range, which is unlikely to be testable at the LHC.

6 Summary and conclusions

In this work we have reconsidered a simple model which contains two new spin-1 states, supposed to be composite together with the Higgs boson, pointing out to a strong dynamical origin of the Electroweak scale. We used dijet data from ATLAS to set limits on the mass of the new states. We found that current data allows masses in the range $2.2 \text{ TeV} \lesssim M \lesssim 4\pi v \approx 3.1 \text{ TeV}$.

Then, we computed $\Gamma(h \rightarrow \gamma\gamma)$ and compared with the SM prediction. We found that our result is compatible with recent measurements at the LHC. In this sense we can say that this simple model has passed the experimental test. This success is related to the fact that in our model the Higgs boson is weakly coupled to the new spin-1 states. This is a consequence of choosing $f_1 = f_2 = 0$ in Eq. (11). The original motivation for this choice was to simplify the model and make sure we could faithfully reproduce the phenomenology of the W^\pm and Z bosons. Nevertheless, we see the agreement with the measured value of R_γ as a posteriori justification.

Unfortunately, on the other hand, the proposed enhancement in the Higgs-strahlung channels has not survived as an important signal of the model at the LHC.

Acknowledgements A.R.Z. has received financial support from Fondecyt grant No. 1120346. O.C.-F. was supported by Fondecyt grant No. 11000287 and Basal Project FB0821. C.C., G.M., F.R. and J.Z. received support from Conicyt National Ph.D. Fellowship Program.

References

1. G. Aad et al. (ATLAS Collaboration), Observation of a new particle in the search for the Standard Model Higgs boson with the ATLAS detector at the LHC. Phys. Lett. B **716**, 1 (2012). [arXiv:1207.7214](#) [hep-ex]
2. S. Chatrchyan et al. (CMS Collaboration), Observation of a new boson at a mass of 125 GeV with the CMS experiment at the LHC. Phys. Lett. B **716**, 30 (2012). [arXiv:1207.7235](#) [hep-ex]
3. E. Hardy, Is natural SUSY natural? [arXiv:1306.1534](#) [hep-ph]
4. R. Foadi, M.T. Frandsen, T.A. Ryttov, F. Sannino, Minimal walking technicolor: set up for collider physics. Phys. Rev. D **76**, 055005 (2007). [arXiv:0706.1696](#) [hep-ph]
5. T.A. Ryttov, F. Sannino, Ultra minimal technicolor and its dark matter TIMP. Phys. Rev. D **78**, 115010 (2008). [arXiv:0809.0713](#) [hep-ph]
6. F. Sannino, Conformal dynamics for TeV physics and cosmology. Acta Phys. Pol. B **40**, 3533 (2009). [arXiv:0911.0931](#) [hep-ph]
7. A. Doff, E.G.S. Luna, A.A. Natale, The 125 GeV boson: a composite scalar? Phys. Rev. D **88**, 055008 (2013). [arXiv:1303.3248](#) [hep-ph]
8. N. Arkani-Hamed et al., J. High Energy Phys. **0208**, 021 (2002). [hep-ph/0206020](#)
9. N. Arkani-Hamed, A. Cohen, E. Katz, A. Nelson, J. High Energy Phys. **0207**, 034 (2002). [hep-ph/0206021](#)
10. M. Schmaltz, D. Tucker-Smith, Annu. Rev. Nucl. Part. Sci. **55**, 229 (2005). [hep-ph/0502182](#)
11. M. Perelstein, Prog. Part. Nucl. Phys. **58**, 247 (2007). [hep-ph/0512128](#)
12. M. Perelstein, M.E. Peskin, A. Pierce, Phys. Rev. D **69**, 075002 (2004). [hep-ph/0310039](#)
13. D.B. Kaplan, H. Georgi, Phys. Lett. B **136**, 183 (1984)
14. S. Dimopoulos, J. Preskill, Nucl. Phys. B **199**, 206 (1982)
15. T. Banks, Nucl. Phys. B **243**, 125 (1984)
16. D.B. Kaplan, H. Georgi, S. Dimopoulos, Phys. Lett. B **136**, 187 (1984)
17. H. Georgi, D.B. Kaplan, P. Galison, Phys. Lett. B **143**, 152 (1984)
18. H. Georgi, D.B. Kaplan, Phys. Lett. B **145**, 216 (1984)
19. M.J. Dugan, H. Georgi, D.B. Kaplan, Nucl. Phys. B **254**, 299 (1985)

20. G.F. Giudice, C. Grojean, A. Pomarol, R. Rattazzi, J. High Energy Phys. **0706**, 045 (2007). [hep-ph/0703164](#)
21. C. Csaki, A. Falkowski, A. Weiler, J. High Energy Phys. **0809**, 008 (2008). [arXiv:0804.1954](#)
22. R. Contino, [arXiv:1005.4269](#)
23. R. Barbieri et al., [arXiv:1211.5085](#)
24. B. Keren-Zur et al., Nucl. Phys. B **867**, 429 (2013). [arXiv:1205.5803](#)
25. A.R. Zerwekh, Associate Higgs and gauge boson production at hadron colliders in a model with vector resonances. Eur. Phys. J. C **46**, 791 (2006). [hep-ph/0512261](#)
26. A. Belyaev, R. Foadi, M.T. Frandsen, M. Jarvinen, F. Sannino, A. Pukhov, Technicolor walks at the LHC. Phys. Rev. D **79**, 035006 (2009). [arXiv:0809.0793](#) [hep-ph]
27. B. Bellazzini, C. Csaki, J. Hubisz, J. Serra, J. Terning, Composite Higgs sketch. J. High Energy Phys. **1211**, 003 (2012). [arXiv:1205.4032](#) [hep-ph]
28. M. Gintner, J. Juran, A 125 GeV scalar improves the low-energy data support for the top-BESS model. [arXiv:1301.2124](#) [hep-ph]
29. A.E. Carcamo Hernandez, C.O. Dib, A.R. Zerwekh, The effect of composite resonances on Higgs decay into two photons. [arXiv:1304.0286](#) [hep-ph]
30. T. Abe, R. Kitano, Phenomenology of partially composite standard model. Phys. Rev. D **88**, 015019 (2013). [arXiv:1305.2047](#) [hep-ph]
31. H. Cai, Higgs-Z-photon coupling from effect of composite resonances. [arXiv:1306.3922](#) [hep-ph]
32. D. Bunk, J. Hubisz, B. Jain, Higgs decays in gauge extensions of the standard model. [arXiv:1309.7988](#) [hep-ph]
33. M. Gintner, J. Juran, The vector resonance triplet with the direct coupling to the third quark generation. Eur. Phys. J. C **73**, 2577 (2013). [arXiv:1309.6597](#) [hep-ph]
34. R.S. Chivukula, E.H. Simmons, H.J. He, M. Kurachi, M. Tanabashi, Phys. Rev. D **71**, 115001 (2005). [arXiv:hep-ph/0502162](#)
35. R. Casalbuoni, S. De Curtis, D. Dominici, R. Gatto, Phys. Lett. B **155**, 95 (1985)
36. R. Casalbuoni, S. De Curtis, D. Dominici, R. Gatto, Nucl. Phys. B **282**, 235 (1987)
37. R. Casalbuoni, P. Chiappetta, A. Deandrea, D. Dominici, R. Gatto, Z. Phys. C **60**, 315 (1993)
38. R. Casalbuoni, P. Chiappetta, S. De Curtis, F. Feruglio, R. Gatto, B. Mele, J. Terron, Phys. Lett. B **249**, 130 (1990)
39. R. Casalbuoni, P. Chiappetta, M.C. Cousinou, S. De Curtis, F. Feruglio, R. Gatto, Phys. Lett. B **253**, 275 (1991)
40. L. Antichini, R. Casalbuoni, S. De Curtis, Phys. Lett. B **348**, 521 (1995)
41. D. Dominici, Riv. Nuovo Cimento **20**, 1 (1997). [arXiv:hep-ph/9711385](#)
42. A. Semenov, LanHEP—a package for automatic generation of Feynman rules from the Lagrangian. Updated version 3.1. [arXiv:1005.1909](#) [hep-ph]
43. A. Belyaev, N.D. Christensen, A. Pukhov, Comput. Phys. Commun. **184**, 1729 (2013). [arXiv:1207.6082](#) [hep-ph]
44. (ATLAS Collaboration), Search for new phenomena in the dijet mass distribution updated using 13.0 fb⁻¹ of pp collisions at $\sqrt{s} = 8$ TeV collected by the ATLAS detector. ATLAS-CONF-2012-148
45. (ATLAS Collaboration), ATLAS-CONF-2013-014
46. (CMS Collaboration), CMS-PAS-HIG-13-005